NANO LETTERS

2009
Vol. 9, No. 9
3137-3141

Fabrication of Ultralong and Electrically Uniform Single-Walled Carbon Nanotubes on Clean Substrates

Xueshen Wang,[†] Qunqing Li,[*,†] Jing Xie,[†] Zhong Jin,[‡] Jinyong Wang,[‡] Yan Li,[‡] Kaili Jiang,[†] and Shoushan Fan[†]

Department of Physics and Tsinghua-Foxconn Nanotechnology Research Center, Tsinghua University, Beijing 100084, People's Republic of China, and College of Chemistry and Molecular Engineering, Peking University, Beijing 100871, People's Republic of China

Received April 20, 2009; Revised Manuscript Received June 12, 2009

ABSTRACT

We report the controlled growth of ultralong single-wall carbon nanotube (SWNT) arrays using an improved chemical vapor deposition strategy. Using ethanol or methane as the feed gas, monodispersed Fe−Mo as the catalyst, and a superaligned carbon nanotube (CNT) film as the catalyst supporting frame, ultralong CNTs over 18.5 cm long were grown on Si substrates. The growth rate of the CNTs was more than 40 μm/s. No catalyst-related residual material was found on the substrates due to the use of a CNT film as the catalyst supporting frame, facilitating any subsequent fabrication of SWNT-based devices. Electrical transport measurements indicated that the electrical characteristics along a single ultralong SWNT were uniform. We also found that maintaining a spatially homogeneous temperature during the growth process was a critical factor for obtaining constant electrical characteristics along the length of the ultralong SWNTs.

Because of the unique mechanical, electrical, and optoelectronic properties, the growth of ultralong and horizontally aligned single-wall carbon nanotube arrays on a substrate has attracted intensive attention in recent years. Various growing methods based on chemical vapor deposition (CVD) have been developed for growing horizontally aligned ultralong SWNTs. External electric field directed growth CVD was utilized to align the SWNTs.[1] Floating catalysts[2] and fast-heating[3,4] CVD were developed to grow millimeter-long SWNTs. An ultralow gas flow CVD strategy was used to grow large-scale horizontally aligned SWNT arrays.[5] Single-crystal quartz was widely adopted to grow dense and highly aligned SWNT arrays due to its contribution to lattice guidance and atomic step.[6−10] The electrical properties of ultralong SWNTs have been studied by several groups.[11−13] Integrated logic circuits have been assembled on one long SWNT. SWNTs have been used in a scalable way for practical devices and circuits, for example, nanotube transistor radios or RF devices have been studied.[14,15] However, the full potential of nanotubes for nanoelectronic applications will not be realized until the growth of SWNTs can be further optimized and controlled.

One challenge is assuring that all of the assembled SWNT-based devices have equivalent properties. While it may seem reasonable to believe that SWNT-FET devices built from one ultralong SWNT are identical, we found that even for one SWNT, it was difficult to ensure equivalent electrical properties from the beginning of the tube to the end because these properties were easily affected by the growth conditions. For example, using the CVD method, there were several factors that played important roles in the growth of CNTs. It was reported that even if the catalyst particles remained unchanged, a change in temperature during SWNT growth led to a consistent variation in diameter and chirality.[16]

Here, we reported the use of an 86 cm long electrical thermal furnace with a constant temperature zone about 25 cm long, from which we obtained ultralong SWNTs up to 18.5 cm long. With an additional supporting frame for the monodispersed catalyst, the substrate was free from catalyst residuals on the substrate and remained clean for the subsequent SWNT-FET fabrication process. We fabricated over 100 SWNT-FET devices with identical electrical properties on one such ultralong SWNT.

We used monodispersed Fe−Mo nanoparticles as catalysts, which were prepared by the method similar to that in ref 17, and their average diameter was about 6.1 nm. A p-doped Si wafer with a thick layer of thermally grown Si dioxide was used as the substrate. On to this, we drew a 3 mm wide single layer of superaligned CNT film[18,19] and laid this film

* To whom correspondence should be addressed. Tel.: +86 10 62796019. Fax: +86 10 62792457. E-mail: QunqLi@tsinghua.edu.cn.
[†] Tsinghua University.
[‡] Peking University.

10.1021/nl901260b CCC: $40.75
Published on Web 08/03/2009

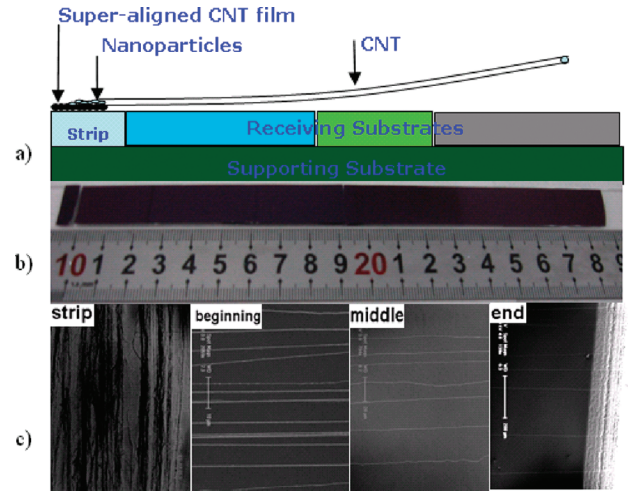

Figure 1. (a) Schematic of the growth method of ultralong CNTs. The catalysts were deposited on a superaligned CNT film which was laid over a strip of silicon, and the catalyst nanoparticles were on the surface of the film. CNTs could be lifted up and caught by the laminar gas flow, and then, they grew in the direction parallel to the gas flow direction. Two or more pieces of SiO_2/Si substrates could be used to accept the CNT array simultaneously. The quartz glass was below the silicon chip as the support. (b) The optical images of an ultralong CNT array. (c) The SEM images of the strip and the beginning, middle, and end of the ultralong CNT array from left to right. The CNTs could cross the slit between the receiving substrates. We can see that some of the CNTs stopped growth and settled to the surface of the substrates during the growth process and became sparse at the end of the substrate.

over the surface of one end of the substrate as the catalyst supporting frame We then immersed this end into catalyst solutions or dropped the catalyst solution onto this strip to transfer the monodispersed nanoparticles to the surface of the CNT film (see Figure s1 and Figure s2 in Supporting Information for details). After ultraviolet treatment to remove the organic solvent, the wafer was put into a 3 in. quartz tube that was heated by a horizontally mounted electrical thermal furnace, as shown in Figure 1. Control valves and standard mass flow controllers were installed so that the feed gas could be switched between two mixtures, (i) a mixture of methanol (CH_4) and hydrogen (H_2) and (ii) a mixture of water vapor, ethanol, and H_2. The furnace temperature was ramped to the desired reaction temperature (830 to 990 °C) within 20 min in an atmosphere of Ar flowing at a rate of 500 sccm, following which the catalyst was treated in 600 sccm H_2 for 10 min. Finally, for the growth of CNTs, the feed gas was introduced at ambient pressure for a time ranging from a few minutes to 1 h.

The ultralong CNTs shown in Figure 1 were grown at 950 °C using ethanol and water as feed gases and Fe−Mo nanoparticles as the catalyst. For 1 h, H_2 flowed through the ethanol (80 mL) and water (20 mL) mixture at 250 sccm to promote the process. The role of water in the growth of CNTs was discussed by Iijima et al.[20] Water can promote and preserve catalytic activity and removed amorphous carbon to aid the growth of vertically aligned nanotube forests. In this work, by adding deionized water to ethanol, we found that water can also promote the growth of CNTs on the substrate. We tried different mixtures of ethanol and deionized water under identical growth conditions and found that a ratio of 4:1 (ethanol/water in volume) worked best.

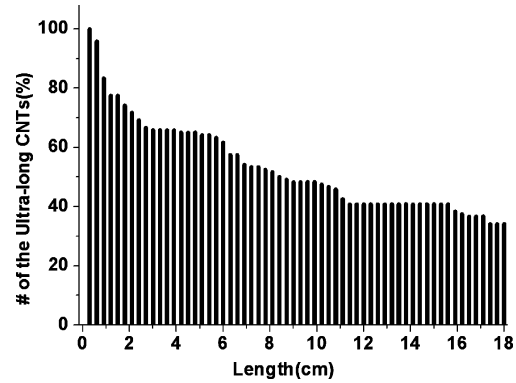

Figure 2. The CNT density variation on a 10 cm long substrate sample. Not all of the CNTs have the maximum length, and about one-three of the ultralong CNTs can reach the end of the substrate.

We further found that if we directly transferred the catalyst nanoparticles to one end of the substrate surface without the help of supporting frame, the CNTs grew only several centimeters long. In addition, in the catalyst area, there would be a lot of amorphous carbon, random short nanotubes, impurity from the catalyst solution, and catalyst congregations which would not act as catalysts for CNT growth. We called all of these materials the catalyst-related residual materials, which make the surface of the substrate unclean. To avoid this, a separate Si substrate was used to receive the resulting CNT arrays (Figure 2a). Using this technique, we found that the CNTs grew much longer than before.

We used two contiguous SiO_2 (500 nm)/Si substrates to collect the ultralong CNTs. CNTs longer than 18.5 cm were grown on the substrates, as shown in Figure 1b. Figure 1c showed SEM images of the CNT sections at the beginning, middle, and end of the receiving substrate. This demonstrated that the CNTs grew across the trenches between the substrates, implying that CNT length was not limited by substrate size. However, as can be seen from Figure 1c, not all CNTs reached the end of the ultralong stage. The CNT density gradually reduced with distance, and many CNTs did not reach the maximum length. Figure 2 gives the CNT density variation of the ultralong CNTs array along a 10 cm long substrate; the CNTs were counted within the substrate width of 1.5 cm. AFM measurement showed that the diameters of aligned CNTs which reached the end were between 1.0 and 2.7 nm (the AFM image is provided in the Supporting Information in Figure s3). Furthermore, the CNTs remained on the substrates after separating two contiguous substrates, which proved advantageous if separate substrates were used, one for catalyst support and one for CNT deposition. Thus, any subsequent fabrication process and the characteristics of any eventual CNT-based devices were free from catalyst pollution.

Since the parallel aligned SWNT density was low, it was possible to integrate a series of individual SWNT-FET devices on one ultralong SWNT. Using photolithographic

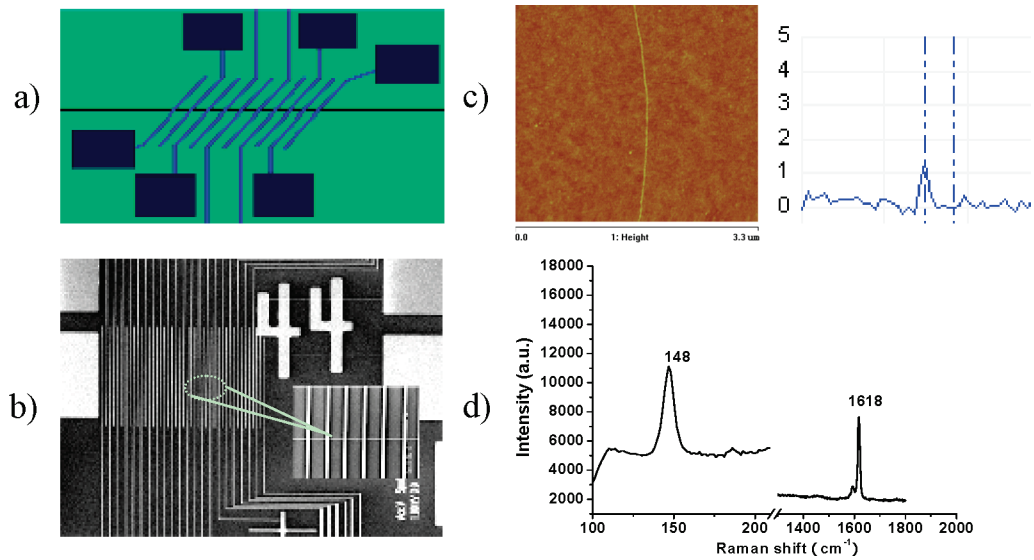

Figure 3. The SWNT-FET array on a single SWNT made by photolithography and electron beam lithography. (a) The schematic of the FET array units. (b) The SEM image of FETs array. The inset is the enlarged view of the dashed circle. (c) The AFM image and AFM height profile of the SWNT. (d) The Raman spectrum of the SWNT.

methods, we fabricated arrays of electrode pads and connected them to the SWNTs with contact lines 200 nm wide and 2 μm apart fabricated by E-beam lithography. Figure 3a shows the device scheme for measuring the electrical characteristics of a 3 cm long SWNT that was grown at 950 °C using ethanol and water as feed gases and Fe−Mo nanoparticles as the catalysts. The diameter of the SWNT was measured by AFM to be 1.36 nm, shown in Figure 3c. Figure 3d reveals the Raman spectrum of this SWNT. The 200 nm wide Cr (10 nm)/Pt (50 nm) connecting lines acted as the source and drain, and the p-doped Si substrate acted as the back gate. After deposition, the contacts were annealed at 400 °C in a mixture of Ar (300 sccm) and H_2 (300 sccm). As shown in Figure 3b, we fabricated in one unit more than 10 SWNT-FET devices, each with a channel length of 2 μm using the E-beam technique. Furthermore, the channel length may be varied simply by choosing different contact pads as the source and drain. Along the 3 cm SWNT, we obtained over 100 SWNT-FET devices.

Electrical homogeneity is very important for using SWNTs to fabricate circuits on a large scale. We characterized over 100 SWNT-FET devices from one end to the other of the 3 cm SWNT, and Figure 4a−d shows the electrical characteristics of a typical device among them. The maximum current reached an average of 17.7 μA at $V_{gs} = -20$ V and $V_{ds} =$ 10 V. The on/off ratio of all devices measured was approximately 10^6, as shown in Figure 4a. Figure 4b showed a typical current (I_{ds}) versus bias voltage (V_{ds}) characteristics for a SWNT-FET device under a different back-gate voltage (V_{gs}). Figure 4c showed the low-bias conductance G of the device as a function of V_{gs}. The carrier mobility in the SWNT has been given as

$$\mu = \frac{L}{C_g V_{ds}} \frac{\partial I_{ds}}{\partial V_{gs}} \quad (1)$$

where C_g is the capacitance per unit length for a semiconducting tube and V_{gs} is the gate voltage. C_g was estimated to be 0.14 pF/cm for our device as it scaled with diameter according to $C_g^{-1} \propto \ln(1 + 2\lambda/d)$, where $\lambda = 500$ nm was the oxide thickness.[21] We calculated the device effective field effect mobility at the linear region of the low-bias conductance. We found average values of approximately 800 cm^2/(V s) at room temperature, which was higher than those of general semiconductors, with the channel length of 2 μm. However, the device resistance was contributed to by the intrinsic CNT resistance and the contact resistance. The resistance of the SWCNT at room temperature under the linear on-state was about 35 kΩ, which was obtained by four point measurement, and the contact resistance was about 232 kΩ. Taking the contact resistance into account and subtracting its effect, the field effect mobility can reach about 10500 cm^2/(V s) for this SWNT. We also measured the electrical properties of SWNT-FET devices with different SWNT diameters and found that the mobility increased with the diameter of the SWNT, and this was similar to the result of the literature[21] (see Figure 4d).

Thus, we found that the electrical properties of the devices measured were uniform along a single SWNT. Figure 5 showed that the average field effect mobility and I_{dsmax} along the length of the SWNT were very stable from one end to the other. Upon changing the channel length by fixing one pad as the drain and selecting different pads as the source, we found the on/off ratio of all SWNT-FET devices to be 10^6.

The kite mechanism proposed by Jie Liu et al.[22] suggested that if SWNTs leave the substrate upon growing, they can be carried by gas flow and may thus grow very long and be directed. The direction and placement of the SWNT arrays were determined by the feed gas flow. It was thought that in order to grow long carbon nanotube, the nanotube should grow above the substrate surface because strong van der

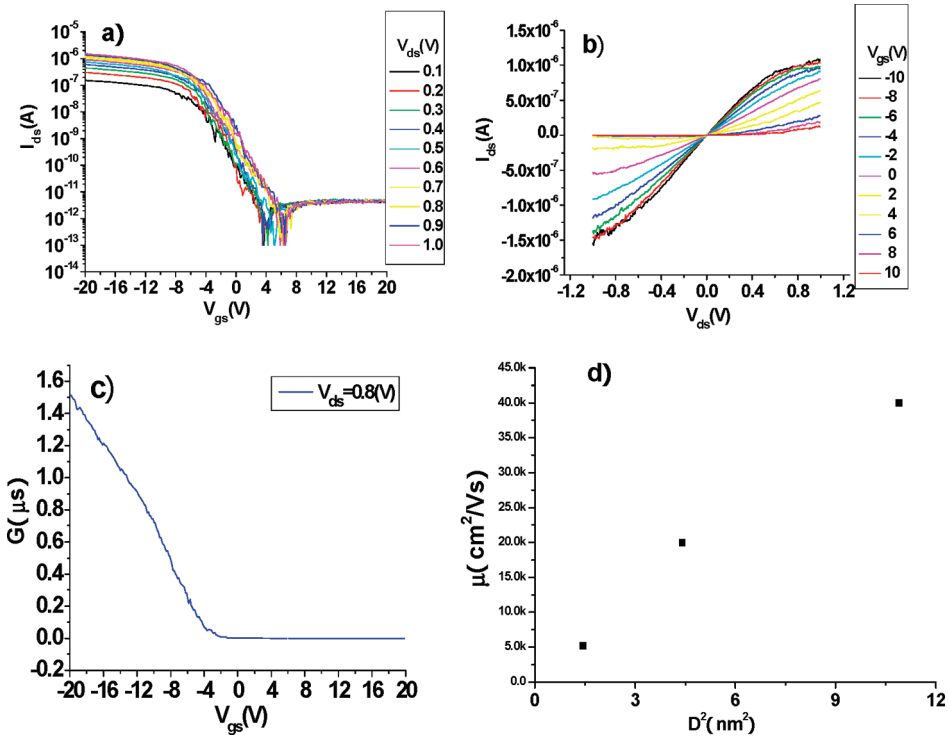

Figure 4. Electrical properties of one typical SWNT-FET device. (a) Current (I_{ds}) versus gate voltage (V_{gs}) characteristics for V_{ds} ranging from 0.1 to 1.0 V, showing that the on/off ratio is about 10^6 at this bias region. (b) Current (I_{ds}) versus bias voltage (V_{ds}) characteristics for V_{gs} ranging from −10 to 10 V. (c) Conductance of this device as a function of V_{gs}. (d) The average mobility versus the square of the diameter of SWNTs with a channel length of 20 μm; the effects of contact are subtracted.

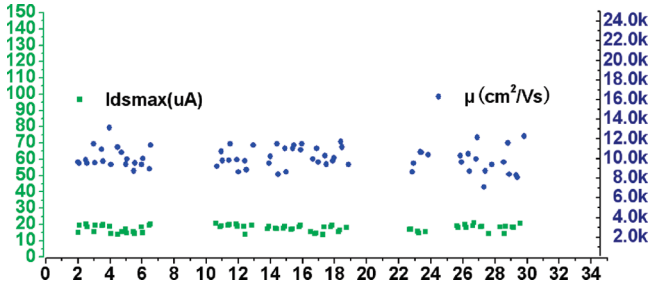

Figure 5. The electrical properties along a 3 cm long SWNT with a diameter of 1.36 nm. Green square: the I_{dsmax} (V_{ds} = 10 V, V_{gs} = −20 V) of the SWNT devices fabricated along this SWNT with a channel length of 2 μm and 200 nm wide Cr (10 nm)/Pt (50 nm) as source and drain pads. Blue circle: the mobility of those SWNT devices (V_{ds} = 1 V, V_{gs}= −20 V); the effects of the contact are subtracted.

Waals interactions between the nanotubes and surface may hinder the smooth growth of the nanotube.[23,24] In our work, we used a superaligned CNT film to support the catalyst. One layer of the superaligned CNT film was about 100 nm thick and provided a step above the substrate. CNTs grown from the catalyst nanoparticles could easily suspend over the substrate and continually grew in the direction of the gas flow without interaction between the tubes and substrate surface. Upon terminating the growth process, CNTs descended onto the substrate, and perturbed CNTs during this descent resulted in curved CNTs winding over the substrate surface.

CNTs can grow over trenches and a superaligned CNT film, and the wide gap between two substrates can be crossed. We demonstrated that CNTs can grow from one substrate to another and longer than 18 cm by growing CNTs over two 10 cm × 2 cm SiO_2/Si receiving substrates placed side by side. When the receiving substrates were separated, the CNTs broke, and the ends recoiled back to the edge of their respective substrate (see Figure s5 in the Supporting Information). This phenomenon may explain why CNTs can sustain perturbations during the fabrication process while CNTs on polluted substrates mostly disappeared after photolithography and the lift-off process. It may indicate that the interactions between the CNT and a clean substrate are slightly higher than those for a polluted substrate. Thus, we can fabricate SWNT-based devices directly, facilitating the device fabrication process.

We also found that maintaining a spatially homogeneous temperature during the growth process was a critical factor for fabricating ultralong SWNTs with consistent electrical characteristics. We found that the growth of SWNTs stopped when a drastic temperature variation occurred, making a long furnace essential for growing ultralong CNT arrays. Moreover, we found that sections of SWNTs grown under different temperatures had different electrical characteristics (see Figure s6 in Supporting Information for details). Only ultralong SWNTs grown under constant temperature showed constant characteristics. In addition, the electrical characteristics of SWNTs may not be constant along the tube if the growth conditions (i.e., gas flow, temperature, etc.) are not stable during growth. For this reason, we used a furnace with a long constant-temperature zone to avoid temperature

fluctuations and carefully controlled gas flow to avoid gas fluctuations at the substrate.

In summary, we have demonstrated the controlled growth of ultralong CNT arrays using monodispersed Fe−Mo nanoparticles as catalysts. Using ethanol or methane as the feed gas and a superaligned CNT film as the supporting frame for catalysts, ultralong CNTs can be grown over 18.5 cm long on substrates. Using E-beam lithography to define FET arrays on one SWNT, we find uniform electrical characteristics over the entire length. Maintaining a spatially homogeneous temperature during the growth period is a critical factor for fabricating ultralong SWNTs with spatially constant electrical characteristics. Further efforts are ongoing to fabricate ultralong SWNT arrays with controlled diameters and to make use of the arrays to manufacture functional devices.

Acknowledgment. This work was supported by the National Basic Research Program of China (2007CB935301, 2005CB623606). We sincerely thank Lihui Zhang and Mo Chen for E-beam lithography and Changqing Yin for the E-beam evaporation for the fabrication of the FET devices. We also thank Chunxiang Luo and Kai Liu for their help.

Supporting Information Available: Methods and materials and additional images. This material is available free of charge via the Internet at http://pubs.acs.org.

References

(1) Zhang, Y. G.; Chang, A. L.; Cao, J.; Wang, Q.; Kim, W.; Li, Y. M.; Morris, N.; Yenilmez, E.; Kong, J.; Dai, H. *J. Appl. Phys. Lett.* **2001**, *79*, 3155.
(2) Huang, S. M.; Cai, X. Y.; Du, C. S.; Liu, J. *J. Phys. Chem. B* **2003**, *107*, 13253.
(3) Huang, S. M.; Cai, X. Y.; Liu, J. *J. Am. Chem. Soc.* **2003**, *125*, 5636.
(4) Huang, S. M.; Maynor, B.; Cai, X. Y.; Liu, J. *Adv. Mater.* **2003**, *15*, 1651.
(5) Jin, Z.; Chu, H. B.; Wang, J. Y.; Hong, J. X.; Tan, W. C.; Li, Y. *Nano Lett.* **2007**, *7*, 2073.
(6) Kocabas, C.; Hur, S. H.; Gaur, A.; Meitl, M. A.; Shim, M.; Rogers, J. A. *Small* **2005**, *1*, 1110.
(7) Kang, S. J.; Kocabas, C.; Ozel, T.; Shim, M.; Pimparkar, N.; Alam, M. A.; Rotkin, S. V.; Rogers, J. A. *Nat. Nanotechnol.* **2007**, *2*, 230.
(8) Kang, S. J.; Kocabas, C.; Kim, H. S.; Cao, Q.; Meitl, M. A.; Khang, D. Y.; Rogers, J. A. *Nano Lett.* **2007**, *7*, 3343.
(9) Ding, L.; Yuan, D. N.; Liu, J. *J. Am. Chem. Soc.* **2008**, *130*, 5428.
(10) Yuan, D. N.; Ding, L.; Chu, H. B.; Feng, Y. Y.; McNicholas, T. P.; Liu, J. *Nano Lett.* **2008**, *8*, 2576.
(11) Hong, B. H.; Lee, J. Y.; Beetz, T.; Zhu, Y. M.; Kim, P.; Kim, K. S. *J. Am. Chem. Soc.* **2005**, *127*, 15336.
(12) Durkop, T.; Getty, S. A.; Cobas, E.; Fuhrer, M. S. *Nano Lett.* **2004**, *4*, 35.
(13) Li, S. D.; Yu, Z.; Rutherglen, C.; Burke, P. J. *Nano Lett.* **2004**, *4*, 2003.
(14) Kocabas, C.; Kim, H.-S.; Banks, T.; Rogers, J. A.; Pesetski, A. A.; Baumgardner, J. E.; Krishnaswamy, S. V.; Zhang, H. *Proc. Natl. Acad. Sci. U.S.A.* **2008**, *105*, 1405.
(15) Kocabas, C.; Dunham, S.; Cao, Q.; Cimino, K.; Ho, X.; Kim, H.; Dawson, D.; Payne, J.; Stuenkel, M.; Zhang, H.; Banks, T.; Feng, M. S.; Rotkin, V.; Rogers, J. A. *Nano Lett.* **2009**, *9*, 1937.
(16) Yao, Y. G.; Li, Q. W.; Zhang, J.; Liu, R.; Jiao, L. Y.; Zhu, Y. T.; Liu, Z. F. *Nat. Mater.* **2007**, *6*, 283.
(17) Jin, Z.; Li, X. M.; Zhou, W. W.; Han, Z. Y.; Zhang, Y.; Li, Y. *Chem. Phys. Lett.* **2006**, *432*, 177.
(18) Zhang, X. B.; Jiang, K. L.; Feng, C.; Liu, P.; Zhang, L. N.; Kong, J.; Zhang, T. H.; Li, Q. Q.; Fan, S. S. *Adv. Mater.* **2006**, *18*, 1505.
(19) Jiang, K. L.; Li, Q. Q.; Fan, S. S. *Nature* **2002**, *419*, 801.
(20) Hata, K.; Futaba, D. N.; Mizuno, K.; Namai, T.; Yumura, M.; Iijima, S. *Science* **2004**, *306*, 1362.
(21) Zhou, X. J.; Park, J. Y.; Huang, S. M.; Liu, J.; McEuen, P. L. *Phys. Rev. Lett.* **2005**, *95*, 146805.
(22) Huang, S. M.; Woodson, M.; Smalley, R.; Liu, J. *Nano Lett.* **2004**, *4*, 1025.
(23) Huang, L. M.; White, B.; Sfeir, M. Y.; Huang, M. Y.; Huang, H. X.; Wind, S.; Hone, J.; O'Brien, S. *J. Phys. Chem. B* **2006**, *110*, 11103.
(24) Yu, Z.; Li, S. D.; Burke, P. J. *Chem. Mater.* **2004**, *16*, 3414.

NL901260B